

Supplementary information

Assembly of reduced graphene oxides into a three-dimensional porous structure via confinement within robust cellulose oligomer networks

Yuuki Hata,^a Yoshitaka Saito,^b Toshiki Sawada,^{ac} Hidetoshi Matsumoto^b and Takeshi Serizawa^{*a}

^aDepartment of Chemical Science and Engineering and ^bDepartment of Materials Science and Engineering, School of Materials and Chemical Technology, Tokyo Institute of Technology, 2-12-1 Ookayama, Meguro-ku, Tokyo 152-8550, Japan. E-mail: serizawa@polymer.titech.ac.jp

^cPrecursory Research for Embryonic Science and Technology (PRESTO), Japan Science and Technology Agency (JST), 4-1-8 Honcho, Kawaguchi-shi, Saitama 332-0012, Japan

Table of Contents	Page
Fig. S1 AFM images of the raw GOs.	S3
Fig. S2 Photographs of GO dispersions after incubation at 60 °C for 3 d at various pHs.	S3
Fig. S3 ¹ H NMR spectrum of the cellulose oligomers.	S4
Fig. S4 ATR-FTIR absorption spectrum of the products.	S4
Fig. S5 AFM image of the mechanically crushed nanoribbons.	S5
Fig. S6 Photographs of the hybrid gels with 1 mg mL ⁻¹ rGO before and after the reduction reaction.	S5
Fig. S7 Mass spectra of cellulose oligomers before and after the reduction reaction.	S6
Fig. S8 Schematic illustration of the two-electrode system for electrochemical measurements.	S6
Fig. S9 Cyclic voltammograms of the rGO gels produced via only once reduction reaction.	S7
Fig. S10 Charge/discharge curves of the rGO gels.	S7
Table S1 The specific capacitance values of the rGO gels	S7
Fig. S11 Cyclic performance and coulombic efficiency of the rGO gels.	S8
Reference	S8

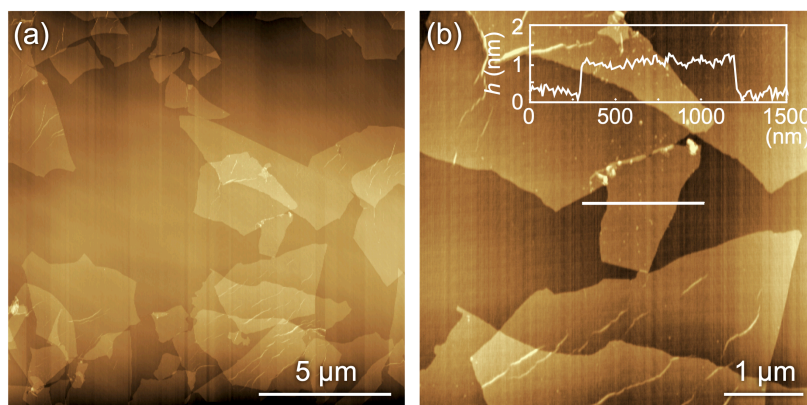


Fig. S1 Atomic force microscopy (AFM) images of the raw graphene oxides (GOs). Inset in (b) is a cross-section.

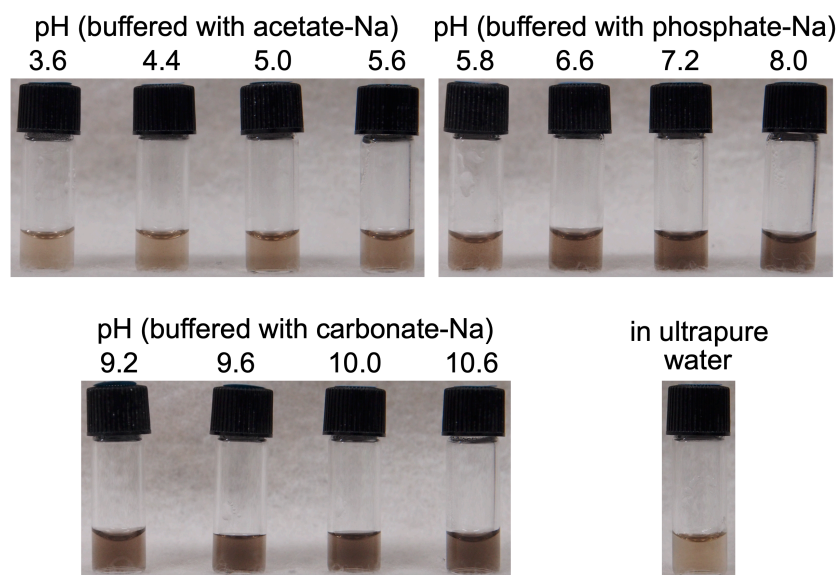


Fig. S2 Photographs of GO dispersions after incubation at 60 °C for 3 d at various pHs. Concentrations of GOs and buffer species were 0.1 mg mL⁻¹ and 0.1 M, respectively. The photographs were taken just after redispersion of GOs by pipetting.

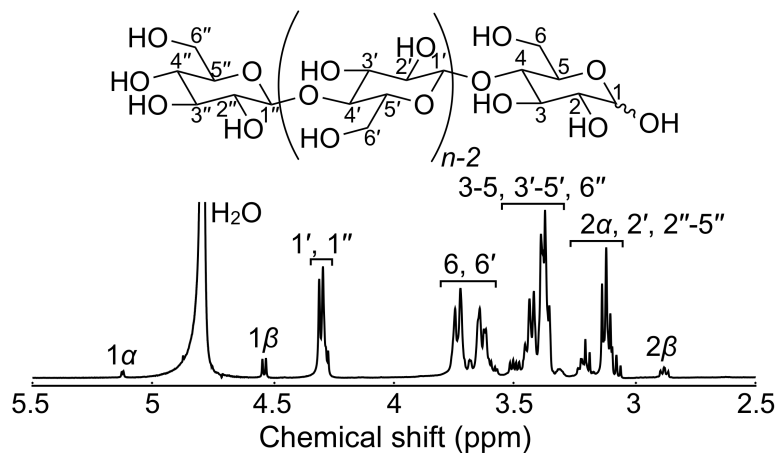


Fig. S3 ¹H NMR spectrum of the cellulose oligomers synthesized in 4 mg mL⁻¹ of GO dispersions.

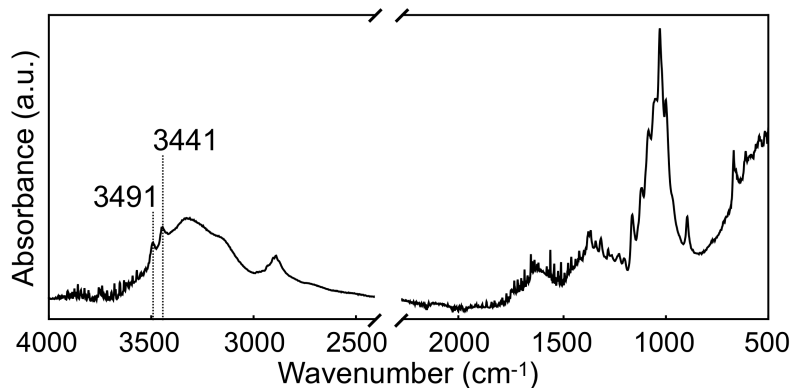


Fig. S4 Attenuated total reflection-Fourier transform infrared (ATR-FTIR) absorption spectrum of the products. The spectrum showed two characteristic peaks for the intrachain hydrogen-bonded hydroxyl groups in the cellulose II allomorph at approximately 3441 and 3491 cm⁻¹.¹

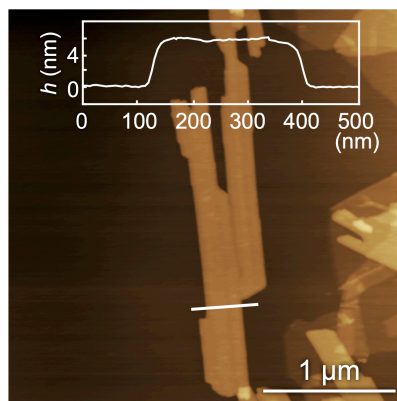


Fig. S5 AFM image of the mechanically crushed nanoribbons. Inset is a cross-section.

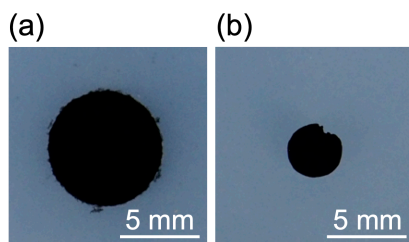


Fig. S6 Photographs of the hybrid gels with 1 mg mL^{-1} reduced GO (rGO) (a) before and (b) after the reduction reaction by hydrogen iodide.

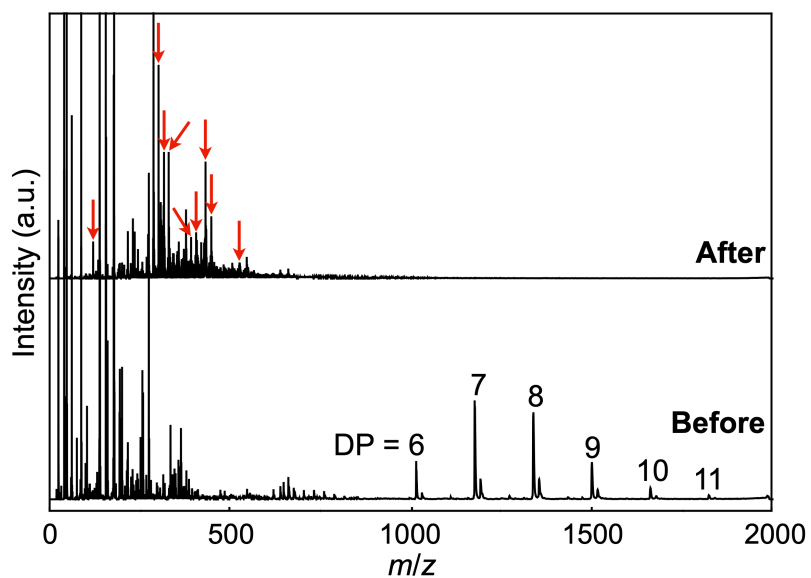


Fig. S7 Matrix-assisted laser desorption/ionization time-of-flight mass spectra of cellulose oligomers before and after the reduction reaction. The numbers above the peaks denote the degree of polymerization (DP) values of the cellulose oligomers. The red arrows indicate newly emerged peaks after the reduction reaction.

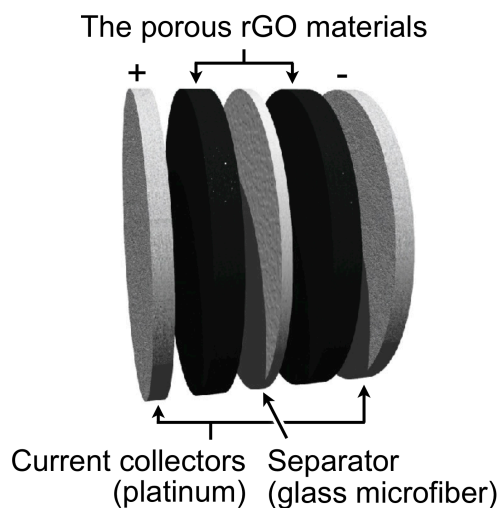


Fig. S8 Schematic illustration of the two-electrode system for electrochemical measurements.

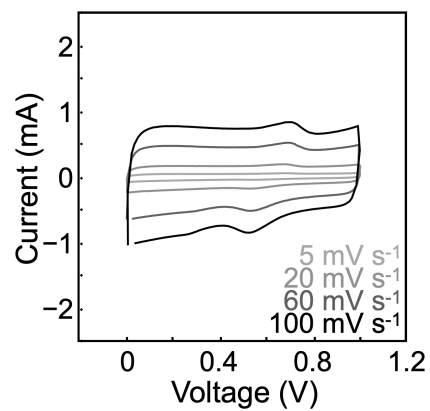


Fig. S9 Cyclic voltammograms of the rGO gels produced via only once reduction reaction.

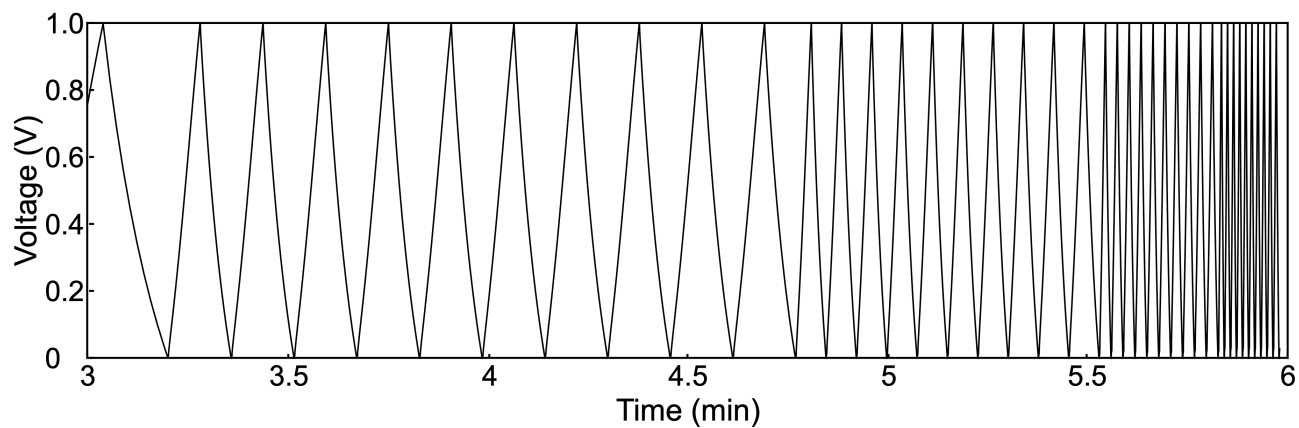


Fig. S10 Charge/discharge curves of the rGO gels after 3 min.

Table S1 The specific capacitance values of the rGO gels

Current density (A g ⁻¹)	5	10	20	50	100
Specific capacitance (F g ⁻¹)	111 ± 10	101 ± 9	96 ± 9	89 ± 8	83 ± 7

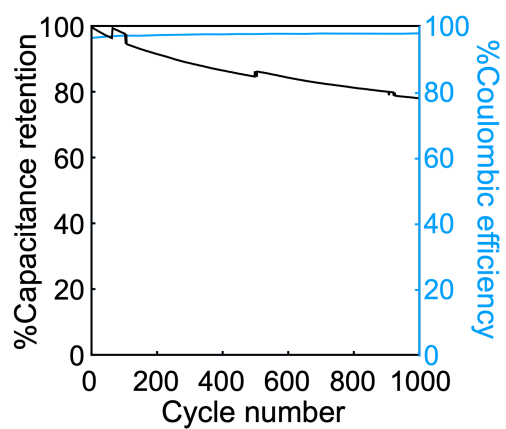


Fig. S11 Cyclic performance and coulombic efficiency of the rGO gels at a current density of 5 A g⁻¹.

Reference

- 1 M. L. Nelson and R. T. O'Connor, *J. Appl. Polym. Sci.*, 1964, **8**, 1311–1324.